Journal of CO_2 Utilization 23 (2018) 80–104

Contents lists available at ScienceDirect

Journal of CO_2 Utilization

journal homepage: www.elsevier.com/locate/jcou

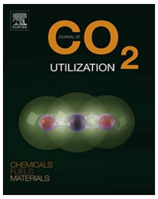

Simulation and optimization of reforming reactors for carbon dioxide utilization using both rigorous and reduced models

Priyadarshini Balasubramanian, Ishan Bajaj, M.M. Faruque Hasan*

Artie McFerrin Department of Chemical Engineering, Texas A&M University, 3122 TAMU, College Station, TX, 77843, USA

ARTICLE INFO

Keywords:
Carbon dioxide utilization
Reactor modeling
Simulation
Surrogate model
Optimization

ABSTRACT

CO_2 is a major greenhouse gas emitted at the global scale from burning fossil fuels. Converting CO_2 to chemicals such as syngas is a promising way to reduce CO_2 emissions from stationary sources. In this work, we explore technologies for the thermochemical conversion of CO_2 to syngas using both rigorous and reduced order reactor models. Specifically, we study the CO_2 utilization potentials of primary reforming such as dry reforming (DR), steam methane reforming (SMR) and partial oxidation (POX), and combined reforming such as combined dry and steam methane reforming (CDSMR), auto-thermal reforming (ATR), combined partial oxidation and dry reforming (PODR) and tri-reforming (TR). Through detailed simulation and analysis, we show the importance of considering rigorous models for accurate prediction. We also develop algebraic surrogate models for reactor outlets as functions of reactor design and operating conditions. The replacement of the high-fidelity models with their simpler algebraic surrogates provides an efficient way for superstructure-based reactor synthesis. Using a mixed-integer nonlinear optimization (MINLP)-based reactor synthesis model, the reactors are further optimized for maximizing CO_2 utilization and syngas selectivity. PODR has been found to have the highest potential for converting CO_2 for the range of syngas ratios (H_2/CO) between 1 and 1.7, achieving almost 100% CO_2 conversion with a syngas selectivity ranging 80–93%. We further improve the conversion and syngas selectivity by distributing the feeds to multiple reformers. A combination of DR, CDSMR and TR achieves the best CO_2 conversion for syngas ratios up to 2.4. For higher syngas ratios, a combination of SMR, TR and RWGS are found to be optimal. These are non-intuitive results that need further attention.

1. Introduction

CO_2 is a major greenhouse gas emitted by human activities at the global scale and its primary source is the burning of fossil fuels. Global CO_2 emissions in 2013 were estimated to be 32.2 $GtCO_2$ [1]. Electricity and heat generation sectors contributed to nearly two-thirds of the stationary emissions. Emissions from electricity generation increased by 50% between 2000 and 2013 [1]. Direct CO_2 emissions from the energy sector are projected to increase from 14.4 $GtCO_2$/year in 2010 to 24–33 $GtCO_2$/year in 2050 [2]. CO_2 capture and storage (CCS) from power plants has gained worldwide interest as a potential measure for climate change mitigation [3], but its wide deployment in industry and power sector is dependent upon substantial cost reduction and suitable storage opportunities [4,5]. In 2010, the U.S. Department of Energy estimated that CCS technologies would add around 80% to the cost of electricity for a new pulverized coal plant, and around 35% to the cost of electricity for a new gasification-based plant [6]. One way to offset this cost is the utilization of the captured CO_2 to produce value-added products [7–11]. A promising route to convert CO_2 is to produce syngas. Syngas is a universal intermediate that can be converted to numerous value-added products like jet fuel, diesel, gasoline, acetic acid, formaldehyde, dimethyl ether (DME), aromatics and olefins via methanol synthesis and Fischer-Tropsch synthesis [12,13].

Fig. 1 shows a compilation of different pathways with syngas as the starting point with the corresponding H_2 to CO ratios (SR) [14–16]. Since syngas can take different paths to produce value-added products, the quality and quantity of syngas becomes a major concern. There are several ways to produce syngas of different qualities. Three primary reactions that produce syngas are dry reforming (DR), steam methane reforming (SMR), and partial oxidation (POX). These reforming reactions and their variants, that either utilize CO_2, produce syngas, or perform both have been discussed in detail in Section 2.

DR produces syngas with H_2 to CO ratios close to one, whereas SMR produces syngas with ratios more than three [17]. Auto-thermal reforming of methane (ATR) and POX produce syngas with H_2 to CO ratios around two [18]. The volumetric ratio of H_2 to (2CO + $3CO_2$)

---

* Corresponding author.
E-mail address: hasan@tamu.edu (M.M.F. Hasan).

https://doi.org/10.1016/j.jcou.2017.10.014
Received 16 July 2017; Received in revised form 12 October 2017; Accepted 13 October 2017

Nomenclature

Abbreviations

ATR	Auto thermal reforming of methane
CCS	Carbon capture and sequestration
CDSMR	Combined dry and steam methane reforming
DR	Dry reforming of methane
FT	Fischer-Tropsch synthesis
HTFT	High temperature Fischer–Tropsch synthesis
LTFT	Low temperature Fischer–Tropsch synthesis
PODR	Combined partial oxidation and dry reforming of methane
POSMR	Combined partial oxidation and steam methane reforming
POX	Partial oxidation of methane
RWGS	Reverse water gas shift
SMR	Steam methane reforming
SR	Syngas ratio
TR	Tri-reforming of methane
WGS	Water gas shift reaction

Symbols

a_{ik}	Number of atoms of element k in species i (–)
a_m	Exterior surface area per unit mass of catalyst ($m^2\ kg_{cat}{}^{-1}$)
A_c	Cross-sectional area of the reactor (m^2)
A_k	Total number of atoms of element k in the reaction mixture (–)
A_p	Surface area of catalyst particle (m^2)
c_{pi}	Specific heat capacity of species i ($J\ mol^{-1}\ K^{-1}$)
d_h	Hydraulic diameter (m)
d_t	Tube diameter (m)
D_i	Diffusivity of species i into the gas mixture ($m^2\ s^{-1}$)
D_p	Diameter of catalyst particle (m)
f	Friction factor (–)
f_i°	Fugacity of pure species i in the standard state (bar)
$\hat{f}_i$	Fugacity of species i in the reaction mixture (bar)
F_i	Molar flowrate of species i (mol/s)
F_i^o	Flowrate of species i at the inlet of the reactor (mol/s)
F_i^{out}	Flowrate of species i at the outlet of the reactor (mol/s)
G_i°	Gibbs free energy of species i in the standard state – $J\ mol^{-1}$)
G^T	Total gibbs energy ($J\ mol^{-1}$)
h_p	Height of catalyst particle (m)
h_s	Particle-fluid heat transfer coefficient ($J\ m^{-2}\ s^{-1}\ K^{-1}$)
ΔH_{298}°	Standard heat of reaction at 298K ($J\ mol^{-1}$)
ΔH_j	Heat of reaction j ($J\ mol^{-1}$)
k_j	Reaction rate constant of reaction j ($mol/s\ kg^{-1}$)
k_{si}	Particle-fluid mass transfer coefficient for species i ($m\ s^{-1}$)
K_i	Adsorption equilibrium constant of species i
L	Length of reactor (m)
MW_i	Molecular weight of species i (kg/mol)
n_i	Composition of species i (–)
N	Number of species in the system (–)
p_i	Partial pressure of gas species i (bar)
P	Pressure (Pa)
Pr	Prandtl number (–)
Q	Reactor external heat duty ($J\ kg^{-1}\ s^{-1}$)
r_j	Rate of reaction j ($mol\ kg_{cat}{}^{-1}\ s^{-1}$)
R	Universal gas constant ($J\ K^{-1}\ mol^{-1}$)
Re	Reynolds number (–)
Sc	Schmidt number (–)
SP, SN	Slack variables (–)
T	Temperature (K)
u_s	Superficial velocity of gases ($m\ s^{-1}$)
V_p	Volume of catalyst particle (m^3)
X_L	Lower bound on variable x
X_U	Upper bound on variable x
z	Length (position) along the reactor bed (m)

Greek letters

μ^v	Total viscosity (Pa s)
μ_i^v	Viscosity of species i (Pa s)
μ_i	Chemical potential of species i ($J\ mol^{-1}$)
ρ_b	Density of catalyst bed (kg/m^3)
$\gamma_{i,j}$	Stoichiometric coefficient of species i in reaction j (–)
ρ_f	Density of fluid/gases (kg/m^3)
ε	Void fraction of catalyst bed (–)
λ_f	Thermal conductivity of fluid ($J\ m^{-1}\ s^{-1}\ K^{-1}$)

Subscripts

f	Bulk fluid conditions
i	Species index
j	Reaction index
k	Element index
l	Index of nonlinear equations
s	Solid conditions

Superscripts

0	Reactor inlet condition
out	Reactor outlet condition
$^\circ$	Standard state condition

also plays an important role in deciding the selectivity of products when High Temperature Fischer-Tropsch (HTFT) synthesis is carried out [15]. Thus, CO_2 can indirectly via syngas or directly with syngas be converted into useful chemicals.

Several works attempted to elucidate CO_2 utilization potential through experimental studies [19–21]. Most of them used heterogeneous catalytic reactions which involve extensive catalyst preparation, pretreatment and regeneration. Experimentation is tedious and expensive. It may not be possible to study all the effects of pressure, temperature and feed composition on the yield and CO_2 utilization, as there are physical limitations to the number of experiments that can be performed. One way to overcome this challenge is to study the reactor systems using computational models that incorporate the phenomena taking place within the reactors and use these models to help understand the extent of CO_2 utilization and syngas production.

Rajesh et al. [22] modeled a SMR reactor using a one-dimensional pseudo-homogeneous model with effectiveness factors and optimized using genetic algorithm for minimum inlet flowrate of CH_4 and maximum output flowrate of CO. Rahimpour et al. [23] used a differential evolution method to optimize a steam reformer using a similar model. Aboosadi et al. [24] optimized a tri-reformer (TR) using a one-dimensional heterogeneous model. Luyben [25] simulated a DR using RGibbs and RPlug models and performed flowsheet optimization to obtain the optimal design parameters for minimum total annualized cost. Swapnesh et al. [26] compared the thermodynamic behavior of CO_2 utilization systems and studied the effects of temperature, pressure and feed ratios. They considered CO_2 hydrogenation to synthesize dimethyl ether (DME) and methane and dry reforming. Noureldin et al. [27] used an equilibrium model to describe different reforming reactors and optimized the utilization process for different objectives. An indicative list of recent works in the modeling, simulation and optimization of reforming-based CO_2 utilization processes is provided in Table 1. An